Received: 14 November 2023 | Revised: 13 June 2024 | Accepted: 15 July 2024

DOI: 10.1002/jbt.23779

RESEARCH ARTICLE

WILEY

Investigating the anticancer properties of six benzothiazolopyrimidine derivatives on colon carcinoma cells, in vitro and in vivo

Melika Bakharzi[1,2] | Elham Attar[1] | Hossein Garmabi[3] | Abbas Ali Esmaeili[3] | Ahmad Reza Bahrami[1,4] | Maryam Danehchin[3] | Maryam M. Matin[1,5]

[1]Department of Biology, Faculty of Science, Ferdowsi University of Mashhad, Mashhad, Iran

[2]Department of Interdisciplinary Oncology, Faculty of Medicine, University of British Columbia, Vancouver, Canada

[3]Department of Chemistry, Faculty of Science, Ferdowsi University of Mashhad, Mashhad, Iran

[4]Industrial Biotechnology Research Group, Institute of Biotechnology, Ferdowsi University of Mashhad, Mashhad, Iran

[5]Novel Diagnostics and Therapeutics Research Group, Institute of Biotechnology, Ferdowsi University of Mashhad, Mashhad, Iran

Correspondence

Maryam M. Matin, Department of Biology, Faculty of Science, Ferdowsi University of Mashhad, Mashhad, Iran.
Email: matin@um.ac.ir

Funding information

Ferdowsi University of Mashhad

Abstract

Colorectal cancer (CRC) is the third most common cancer in the world. Despite considerable improvements in the treatment of this cancer, further research to discover novel and more effective agents is ongoing. In this study, possible cytotoxic and apoptotic properties of six benzothiazolopyrimidine derivatives were studied. To assess the IC_{50} values of these agents, MTT assay was performed on HCT 116, CT26, and NIH/3T3 cells. Moreover, cell death mechanism induced by studied compounds was evaluated by PI/annexin V staining. Then, based on molecular docking results and in vitro experiments, the compounds with the highest anticancer properties were further analyzed in vivo in a mouse model of CRC. MTT results indicated that BTP(1) and BTP(4) had the highest selective cytotoxicity on colorectal cancer cells. Furthermore, flow cytometry results demonstrated a considerable increase in the percentage of the early apoptotic cells in BTP(1)- and BTP(4)-treated groups. In vivo studies confirmed the antitumor properties of the two compounds by a significant regression in tumor size of BTP(1)- and BTP(4)-treated mice compared to control groups. Histopathological examination of tumor tissues showed an increased number of apoptotic cells in these two groups compared to the control animals. Additionally, hematoxylin and eosin staining of the spleen and liver of treated mice did not exhibit considerable tissue damage. Thus, BTP(1) and BTP(4) can be considered promising agents in the treatment of colorectal cancer, although further experiments are required to assess their mechanism of action before their application in clinical studies.

KEYWORDS

anticancer properties, benzothiazolopyrimidine, colorectal cancer, molecular docking, mouse model

Melika Bakharzi and Elham Attar contributed equally to this study.

1 | INTRODUCTION

Cancer is defined as a complex disease associated with dynamic changes in the genome.[1] Colorectal cancer (CRC) is the third most commonly diagnosed malignancy, which ranks second in terms of mortality in the world.[2] Most colorectal cancer deaths are related to liver metastasis.[3] Positive family history, deleterious lifestyle, unhealthy diet, and some diseases have shown strong associations with CRC incidence.[4] Despite the achievements of current chemotherapy in CRC, which includes single/multiple-agent regimens, chemotherapy is suffering from considerable limitations.[5] These constraints including systemic toxicity and unpredictable acquired resistance, necessitate the search for safer anticancer compounds.

Benzothiazole is a bicyclic compound, which has been extensively studied in drug development research.[6] It has exhibited diverse biological properties including anticancer,[7] antimicrobial,[6] antioxidant,[8] anti-inflammatory,[9] fungicidal,[10] and antiviral[7] activities. The benzothiazole nucleus serves as a starting material for the synthesis of a large number of therapeutic agents.[6] Pyrimidine, which is a building block of DNA and RNA, has demonstrated a wide spectrum of anticancer potentials such as anti-neoplastic, antiproliferative, antiangiogenic, and cyclin-dependent kinase inhibitory effects.[11] Pyrimidine fused with benzothiazole, called benzothiazolopyrimidine (BTP), is a group of hybrid heterocyclic compounds with promising anticancer properties.[9,12,13] This view is supported by numerous research papers on benzothiazolopyrimidine derivatives. In Waghmare's study, a benzothiazolopyrimidine derivative indicated excellent growth inhibition against lung cancer, breast cancer, and renal cancer cell lines.[14] Moreover, another study reported that a benzothiazolopyrimidine derivative possessed strong antitumor effects against Colo205, U937, MCF-7, and A549 cancer cell lines.[15] Studying its mechanism of action revealed that this compound induced apoptosis through P53 activation and caused G2/M cell cycle arrest.

SRC homology region 2 (SH2)-containing protein tyrosine phosphatase-2 (SHP2) is a cytoplasmic tyrosine phosphatase encoded by PTPN11.[16] SHP2 plays a role in several signaling cascades associated with cell survival and immune regulation, including the RAS–ERK, PI3K–AKT, JAK–STAT, and PD-1/PD-L1 pathways.[17] Studies indicate that SHP2 dysregulation contributes to the development of various cancers including breast,[18] gastric carcinoma,[19] and non-small cell lung[20] cancers, positioning SHP2 as a potential target for cancer therapy. SHP2 exhibits a multifaceted role in CRC. It has been reported to have tumor-suppressing roles by inhibiting CRC cell proliferation and migration, and negatively regulating the phosphorylation of STAT3.[21] However, it has also been associated with promoting proliferation and oxaliplatin resistance in colon cancer cells.[22] Additionally, SHP2 has been found to mediate tumor immunosuppression in colon cancer via the CD47/SIRPα axis, and its allosteric inhibition has been shown to remodel the antitumor microenvironment.[23] The complexity of SHP2 functions makes it a challenging but important target for therapeutic intervention in CRC.

In the current study, we first examined the molecular docking of six benzothiazolopyrimidine derivatives on SHP2 protein, which was introduced as a probable target of benzothiazolopyrimidine derivatives previously.[24] Moreover, the cytotoxic effects of these compounds were evaluated on HCT 116 colorectal cancer cells, using MTT assay. Then, based on our preliminary results obtained from docking and cytotoxicity assay, the compounds with the highest anticancer activities were selected for further in vitro investigations on CT26 (murine colon carcinoma) and NIH/3T3 (mouse embryonic fibroblast) cells. Apoptotic-inducing effects of the selected compounds were further assessed using propidium iodide (PI)/annexin V staining. Finally, antiproliferative properties of these compounds were evaluated in vivo on tumors developed in BALB/c mice. Figure 1 represents a schematic summary of this study.

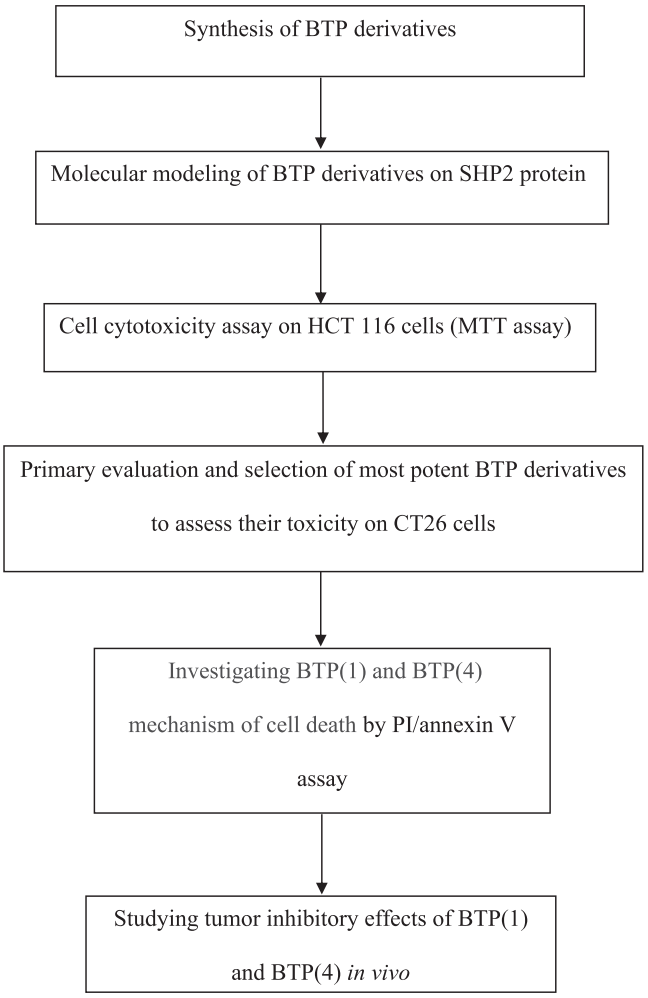

FIGURE 1 Study flowchart.

2 | MATERIALS AND METHODS

2.1 | Synthesis of compounds

BTP derivatives were synthesized as previously described.[24,25] The standard procedure for synthesizing BTPs can be found in the Online

Resource Figure S1. The structural characteristics of these derivatives are as follows:

3-Benzyl-8-chloro-2-hydroxy-4*H*-benzo[4,5]thiazolo[3,2-*a*] pyrimidin-4-one (BTP(1)):

White powder; (0.31 g, 89% yield); mp = 280–282°C; IR(KBr) (υ_{max}/cm^{-1}): υ= 1683 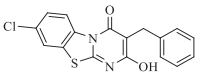 (C = O), 1615 (C = N); ^{1}H NMR (300.13 MHz, DMSO-d_6): δ (ppm) 3.74 (2H, s, CH_2), 7.13(1H, t, J = 7.5 Hz, ArH), 7.23(2H, t, J = 7.5 Hz, ArH), 7.32 (2H, d, J = 6.5 Hz, ArH), 7.45 (1H, dd, J = 1.8 Hz, 9 Hz, ArH), 8.02 (1H, d, J = 2.4 Hz, ArH), 8.81 (1H, d, J = 9 Hz, ArH), 12.03 (1H, s, OH); ^{13}C NMR (76 MHz, DMSO) δ 28.7, 97.5, 119.9, 122.9, 126.0, 127.1, 127.2, 128.4, 128.7, 130.8, 135.4, 141.2, 159.7, 162.2, 164.8; (*m*/*z*, %), 342 (M, 17), 338 (98), 309 (37), 234 (34), 209 (98), 183 (98), 130 (99), 103 (87), 91 (100), 77 (76), 65 (40), 29 (90); Anal. Calcd. for $C_{17}H_{11}ClN_2O_2S$ (342.80): C, 59.56; H, 3.23; N, 8.17; S, 9.35. Found: C, 56.41; H, 3.23; N, 8.08; S, 9.39.

3-(4-Chlorobenzyl)−2-hydroxy-4*H*-benzo[4,5]thiazolo[3,2-*a*] pyrimidin-4-one (BTP(2)):

White powder; (0.32 g, 95% yield); mp=294-296°C; 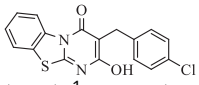 IR(KBr) (υ_{max}/cm^{-1}): υ = 1623 (C=O), 1593 (C=N); ^{1}H NMR (300.13 MHz, DMSO-d_6): δ (ppm) 3.74 (2H, s, CH_2), 7.28-7.34 (4H, m, ArH), 7.48-7.58 (2H, m, ArH), 7.99- 8.03 (1H, m, ArH), 8.94- 8.97 (1H, m, ArH), 12.01 (1H, s, OH); ^{13}C NMR (76 MHz, DMSO) δ; 28.1, 96.9, 118.8, 123.3, 124.1, 126.9, 127.2, 128.5, 130.5, 130.7, 136.6, 140.1, 160.3, 162.7, 164.8. (*m*/*z*, %), 342 (M, 57), 339 (98), 310 (48), 304 (65), 283 (22), 201(65), 176 (100), 164 (97), 149 (98), 124(98), 101 (95), 75(87), 63 (57), 51 (45), 28 (58); Anal. Calcd for $C_{17}H_{11}ClN_2O_2S$ (342.02): C, 59.56; H, 3.23; N, 8.17; S, 9.15%. Found: C, 59.65; H, 3.21; N, 8.06; S, 9.17.

2-Hydroxy-3-(3-hydroxybenzyl)−4*H*-benzo[4,5]thiazolo[3,2-*a*] pyrimidin-4-one (BTP(3)):

White powder; (0.31 g, 96% yield); mp ≥ 300°C; IR(KBr) (υ_{max}/cm^{-1}): υ= 3373 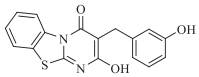 (OH), 1652 (C=O), 1606 (C=N); ^{1}H NMR (300.13 MHz, DMSO-d_6): δ (ppm) 3.69 (2H, s, CH_2), 6.56 (1H, d, J = 9 Hz, ArH), 6.78 (2H, d, J = 6 Hz, ArH), 7.06 (1H, t, J = 7.5 Hz, ArH), 7.45-7.55 (2H, m, ArH), 7.96 (1H, d, J = 7.5 Hz, ArH), 8.94(1H, d, J = 9 Hz, ArH), 9.20 (1H, s, OH), 11.94 (1H, s, OH), ^{13}C NMR (76 MHz, DMSO) δ 28.7, 97.4, 113.1, 115.7, 118.8, 119.6, 123.2, 124.0, 126.8, 127.1, 129.3, 136.5, 142.7, 157.6, 159.7, 162.4, 164.7; (*m*/*z*, %), 324 (M, 8), 321 (82), 202 (10), 176 (100), 149 (80), 107 (60), 77 (45), 65 (40), 40 (22), 29 (50). Anal. Calcd for $C_{17}H_{12}N_2O_3S$ (324.35): C, 62.83; H, 4.36; N, 8.64; S, 9.88%. Found: C, 62.66; H, 4.28; N, 8.49; S, 9.64.

2-Hydroxy-3-(naphthalene-2-ylmethyl)−4*H*-benzo[4,5]thiazolo [3,2-*a*]pyrimidin-4-one (BTP(4)):

Bright Green powder; (0.34 g, 97% yield); mp= 285-287°C; IR (KBr) (υ_{max}/cm^{-1}): υ = 1668 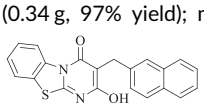 (C=O), 1602 (C=N); ^{1}H NMR (300.13 MHz, DMSO-d_6): δ (ppm) 3.95 (2H, s, CH_2), 7.39–7.47 (2H, m, ArH), 7.50– 7.57 (3H, m, ArH), 7.76 (1H, s, ArH), 7.84 (3H, t, J = 6 Hz, ArH), 7.98 (1H, d, J = 6.8 Hz, ArH), 8.96 (1H, d, J = 6.8 Hz, ArH), 12.14 (1H, s, OH); ^{13}C NMR (76 MHz, DMSO) δ 29.0, 97.1, 118.9, 123.3, 124.0, 125.5, 126.2, 126.3, 126.9, 127.1, 127.7, 127.8, 127.9, 132.0, 133.5, 136.6, 138.9, 160.0, 162.6, 164.9; (*m*/*z*, %), 358 (M, 28), 354 (97), 216 (97), 176 (97), 149 (97), 122 (36), 95 (48), 69 (100), 45 (43), 41 (52), 29 (67). Anal. Calcd. for $C_{21}H_{14}N_2O_2S$ (358.08): C, 70.37; H, 3.94; N, 7.82; S, 8.94%. Found: C, 70.37; H, 3.86; N, 7.75; S, 8.64.

3-(3,4-Dichlorobenzyl)−2-hydroxy-4*H*-benzo[4,5]thiazolo[3,2-*a*] pyrimidin-4-one (BTP(5)):

White powder; (0.35 g, 94% yield); 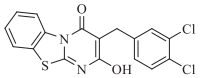 mp = Mp>300°C; IR(KBr) (υ_{max}/cm^{-1}): υ= 1674 (C=O), 1612 (C=N); ^{1}H NMR (300.13 MHz, DMSO-d_6): δ (ppm) 3.74 (2H, s, CH_2), 7.27 (1H, dd, J = 7.2 Hz, 2.1 Hz, ArH), 7.46 (IH, s, ArH), 7.49–7.56 (3H, m, ArH), 7.98 (1H, dd, J = 7.2 Hz, 1.5 Hz, ArH), 8.92 (1H, dd, J = 7.2, 1.5 Hz, ArH), 12.11 (1H, s, OH); ^{13}C NMR (76 MHz, DMSO) δ 28.0, 96.3, 123.3, 124.0, 126.9, 127.1, 128.7, 129.1, 130.1, 130.6, 131.0, 136.5, 142.5, 160.3, 162.4, 164.9; (*m*/*z*, %), 378 (M, 18), 377 (54), 374 (97), 344 (27), 337 (27), 316 (10), 201 (46), 197 (60), 176 (100), 149 (100), 135 (87), 108 (77), 89 (50), 69 (78), 63 (60), 45 (40), 28 (79). Anal. Calcd for $C_{17}H_{10}C_{l2}N_2O_2S$ (377/24): C, 54.13; H, 2.67; N, 7.43; S, 8.50%. Found: C, 54.22; H, 2.57; N, 7.42; S, 8.35.

3-(3-Bromobenzyl)−2-hydroxy-4*H*-benzo[4,5]thiazolo[3,2-*a*] pyrimidin-4-one (BTP(6)):

White powder; (0.36 g, 95% yield); mp = 298–300°C; 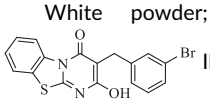 IR(KBr) (υ_{max}/cm^{-1}): υ= 1675 (C=O), 1613 (C=N); ^{1}H NMR (300.13 MHz, DMSO-d_6): δ (ppm) 3.74 (2H, s, CH_2), 7.17 (1H, t, J = 7.5 Hz, ArH), 7.30- 7.35 (2H, m, ArH), 7.46-7.51 (3H, m, ArH), 7.93-7.98 (1H, m, ArH), 8.90-8.95 (1H, m, ArH), 12.05 (1H, s, OH); ^{13}C NMR (76 MHz, DMSO) δ 28.4, 96.7, 118.8, 121.8, 123.2, 124.0, 126.8, 127.1, 127.9, 129.0, 130.6, 131.3, 136.5, 144.2, 160.1, 162.4, 164.8.; (*m*/*z*, %), 386 (M, 43), 304 (6), 207 (8), 176 (100), 149 (70), 102 (65), 90 (48), 76 (23), 50 (12), 28 (48). Anal. Calcd for $C_{17}H_{11}$ BrN_2O_2S (385.25): C, 52.73; H, 2.86; N, 7.23; S, 8.26%. Found: C, 52.73; H, 2.54; N, 7.25; S, 8.26.

2.2 | Molecular docking

The molecular modeling study of compounds BTP(1–6) was carried out using the crystal structure of SHP2 (PDB ID: 5EHR) from RCSB protein data bank (http://www.rcsb.org/pdb). BTP(1–6) were drawn by Chem3D Pro 12.0 and they were optimized for geometry and energy using MM2 force field. The protein structure was prepared by removing water molecules and the original ligand SHP099 (coded as 5OD) by using Discovery Studio software. The protein and compounds BTP(1-6) were prepared by AutoDockTools software (version 1.5.7) by adding polar hydrogens and computing Gasteiger charges. A grid box size of 16 × 16 × 16 dimensions, with a spacing of 1.000 Å was implemented for the SHP2 docking site and was

centered on x, y, and z coordinates (22.586, 41.238, 5.392), where the original binding ligand 5OD was situated.

2.3 | Preparing various concentrations of benzothiazolopyrimidine derivatives

Different concentrations of benzothiazolopyrimidine derivatives were prepared by dissolving 2 mg of each compound in 100 µL dimethyl sulfoxide (DMSO; Merck), and then diluted with complete culture medium before experiments. To increase the accuracy, equal amounts of DMSO (0.5%) were applied to each concentration. Likewise, the viability of each treatment was compared to control DMSO with the same percentage (0.5%).

2.4 | HCT 116, CT26, and NIH/3T3 cell culture

Cell lines were obtained from Ferdowsi University of Mashhad (Mashhad, Iran). HCT 116 and CT26 cells were grown in RPMI 1640 (Gibco) medium supplemented with 10% fetal bovine serum (FBS; Gibco), while NIH/3T3 cells were cultured using low glucose Dulbecco's modified Eagle's medium (LG-DMEM; Gibco) containing 10% FBS. Cells were incubated at 37°C in a humidified atmosphere of 5% CO_2 in the air and sub-cultured using 0.25% trypsin-1 mM EDTA (Tinabshimi) when required.

2.5 | In vitro cytotoxicity assay

To evaluate the cytotoxicity of benzothiazolopyrimidine derivatives, HCT 116, CT26, and NIH/3T3 cells were seeded in 96-well plates (9000 cells/well) (SPL) for 24 h before treatments. Then, cells were incubated with increasing concentrations of compounds ranging from 3.125 to 100 µg/mL for 24, 48, and 72 h. Cisplatin was also considered as a positive control for different assessments. Cellular viability was evaluated by MTT assay. To do so, MTT solution (5 mg/mL in phosphate-buffered saline [PBS]) (Sigma) was added to each well, and after 2 h of incubation, the resulting formazan crystals were solubilized in 150 µL DMSO. The absorption was then measured at 540 nm in an ELISA reader (Awareness Technology, Inc.) and the relative optical density (OD) values were recorded.[26,27] The percentage of living cells compared to the controls was calculated according to the following equation for different treatments:

$$\text{Cell viability (\%)} = [(OD_{mean} \text{ of treated cells} - OD_{mean} \text{ blank})/(OD_{mean} \text{ of control cells (DMSO)} - OD_{mean} \text{ blank})] \times 100.$$

2.6 | Apoptosis detection

Apoptosis was assessed in CT26 cells using fluorescein isothiocyanate (FITC) annexin V apoptosis detection kit with PI (MabTag) according to the manufacturer's instructions.[28] Briefly, treated cells and their relevant controls were washed and collected, suspended in 90 µL annexin V binding buffer, and stained with 5 µL annexin V conjugate and 5 µL PI solution. Then, samples were incubated at 37°C for 20 min, followed by the addition of 400 µL annexin V binding buffer. Samples were spun down at 400*g* for 5 min and resuspended in annexin V binding buffer. Finally, cells were analyzed by flow cytometry (BD-Accuri C6) using FL1 and FL2 channels. To study apoptosis at early stages, a 46 h time interval was selected as a suitable time for staining. Moreover, to set up the flow cytometer instrument three groups of cells including (1) untreated and unstained CT26 cells, (2) cisplatin-treated CT26 cells only stained with annexin V, and (3) cisplatin-treated CT26 cells only stained with PI, were employed. Furthermore, cisplatin as an apoptosis inducing anticancer drug was also studied as a positive control. The results of flow cytometry were analyzed using FlowJo 10.6.2 software.

2.7 | In vivo assays

BALB/c male and female mice were kept and reproduced in the animal house of Ferdowsi University of Mashhad and experiments were performed on their male offspring (20 ± 5 g, 6–8 weeks of age). The animals were fed with free access to a standard chow diet. The mice were maintained at 25 ± 2°C, with a relative humidity of 55 ± 5% and a 12 h light–dark cycle. All experiments were conducted under the FUM-approved codes of the care and use of laboratory animals (IR.UM.REC.1400.052, IR.UM.REC.1400.053).

2.7.1 | Tumor induction and treatments

CT26 cells (2×10^6 cells/100 µL PBS) were implanted subcutaneously in the right flank of mice. When the tumor volume reached 100–300 mm^3 (approximately 10 days after cell injection), animals were randomly divided into seven groups; including PBS group (negative control), DMSO group (solvent control), cisplatin group (positive control), 10 mg/kg body weight BTP(1) or BTP(4), and 50 mg/kg body weight BTP(1) or BTP(4). Each group contained 5 mice and various agents were administered intraperitoneally every other day for 13 days.[27,29]

Tumor volume was regularly estimated before each injection by a digital caliper (Mitutoyo, Japan) with 0.01 mm precision, and calculated using the following formula:

$$\text{Tumor volume} = \text{length} \times \text{width} \times \text{height} \times 0.5.$$

Finally, mice were killed on Day 15, and their tumor, spleen, and liver were removed. Then, tissues were fixed and used for histopathological examinations upon hematoxylin and eosin staining.

2.8 | Statistical analyses

The normal distribution of data was determined by the Shapiro-Wilk test. Significant level was calculated by Student's *t* test (two-tailed) and one-way ANOVA, followed by Tukey multiple comparison test, using GraphPad Prism 8.3.0 software. Values are expressed as mean ± SD or SEM. *p* Values less than 0.05 were considered statistically significant.

3 | RESULTS

The binding energies and types of interactions between SHP2 protein and docked compounds BTP(1-6) were investigated and the results are reported in the Online Resource Table S1. Additionally, Online Resource Figures S2–7 represent two-dimensional and three-dimensional conformations of the docked SHP2 protein with these compounds. Cytotoxic properties of BTP(1-6) on HCT 116 cell line were assessed and the results are demonstrated in Table 1. Among the evaluated benzothiazolopyrimidine derivatives, the highest anticancer activity values on HCT 116 cells were observed for the BTP(1) and BTP(4). Cytotoxic effects of benzothiazolopyrimidine derivatives were compared with cisplatin, a general and well-known anticancer drug, as a positive control (Table 1). dose–response curves are presented in the online Resource Figure S8.

The IC_{50} values of BTP(1) on CT26 cells were calculated as 37.22 μg/mL (108.57 μM), 27.67 μg/mL (80.71 μM), and 12.69 μg/mL (37.01 μM) after 24, 48, and 72 h of treatment, respectively. Moreover, IC_{50} values of 39.8 μg/mL (110.96 μM) after 24 h, 24.7 μg/mL (68.9 μM) after 48 h, and 13.9 μg/mL (38.9 μM) after 72 h of treatment were obtained for CT26 cells treated with BTP(4) (Table 2). On the other hand, treating non-tumorigenic mouse fibroblast NIH/3T3 cells with BTP(1) and BTP(4) resulted in fewer cytotoxic effects compared to CT26 murine colorectal carcinoma cells. The IC_{50} values of BTP(1) on NIH/3T3 cells were estimated as 95.71 μg/mL (279.20 μM), 70.61 μg/mL (205.98 μM), and 67.81 μg/mL (197.81 μM) after 24, 48, and 72 h of treatment, respectively. Similarly, the IC_{50} values of 85.6 μg/mL (238.8 μM), 60.4 μg/mL (168.6 μM), and 59.4 μg/mL (165.6 μM) were calculated for BTP(4) in the mentioned time intervals (Table 2). To compare the cytotoxic effects of the most potent BTP derivatives with cisplatin, CT26 and NIH/3T3 cells were also treated with different concentrations of cisplatin for the same time intervals (Table 2 and Figure 2).

TABLE 1 Antiproliferative activity of BTP derivatives and cisplatin on HCT 116 cells during 24, 48, and 72 h of treatment.

Compounds	C_{50} (μM) ± SEM (HCT 116)		
	24 (h)	48 (h)	72 (h)
BTP(1)	253.52 ± 2.74	221.90 ± 3.50	171.47 ± 3.09
BTP(2)	448.80 ± 31.75	257.44 ± 13.42	180.42 ± 10.58
BTP(3)	337.90 ± 14.67	755.35 ± 35.45	1781.71 ± 22.19
BTP(4)	227.50 ± 1.8	203.51 ± 0.5	146.59 ± 1.5
BTP(5)	366.94 ± 3.3	263.74 ± 1.5	279.30 ± 3.7
BTP(6)	435.30 ± 2.3	290.34 ± 4.2	201.55 ± 3.7
Cisplatin	152.06 ± 14.89	74.76 ± 15.73	63.63 ± 13.16

To further investigate BTP(1) and BTP(4) effects on CT26 cells, the mechanism of cell death was assessed by flow cytometry. The obtained results showed a considerable increase in the percentage of early apoptotic cells in both BTP derivatives and cisplatin-treated groups compared to the controls (Figure 3).

The antitumor effects of selected BTP derivatives were also evaluated in BALB/c mice bearing CT26 colon carcinoma cells. In vivo results demonstrated a significant regression in tumor size of BTP-treated groups compared to the control groups. Examined concentrations of BTP(1) and BTP(4), 10 and 50 mg/kg, as well as cisplatin (5 mg/kg) indicated a remarkable antitumor efficacy compared to control groups (Figure 4).

Histopathological examination of tumor tissues showed an increased number of apoptotic cells in cisplatin-, BTP(1)-, and BTP (4)- (both concentrations) treated groups compared to PBS and DMSO groups. Moreover, to evaluate the cell toxicity of studied compounds, hematoxylin and eosin staining of the liver and spleen was performed in different groups. While normal tissue microstructures were found in all groups, mice treated with 50 mg/kg of BTP(4) and cisplatin developed liver and spleen lesions (Figure 5).

4 | DISCUSSION AND CONCLUSION

About 10% of annual cancer-related deaths are due to colorectal cancer. CRC incidence is anticipated to increase to 2.5 million new cases worldwide in 2035, considering its continuous increase in developing countries.[4] In 2022, 151,030 new CRC cases and 52,580 CRC deaths were estimated to occur in the United States.[30] The main cancer treatment modalities include chemotherapy, radiation, surgery, targeted therapy, and interventional oncology.[31] Cisplatin, as a well-known anticancer agent, is associated with numerous undesirable side effects such as nephrotoxicity, hepatotoxicity, and cardiotoxicity.[32] Due to the serious limitations of available chemotherapeutic agents, the development of new and safer anticancer drugs to improve treatment efficacy is fundamental.

In this study, based on molecular docking analysis, BTP(1) and BTP(4) showed the highest affinities to SHP2 protein with −8.00 and −8.43 kcal/mol values, respectively. BTP(1) exhibited three hydrogen binding interactions with amino acids Asp481, Thr218, and Thr219. It also showed eight hydrophobic interactions with amino acid residues Phe113, Thr219, His114, Pro491, and Leu254. Further, BTP(1) showed three electrostatic interactions with amino acid residue Arg111. BTP(4) exhibited three hydrogen binding interactions with amino acids Thr218, Thr219, and Arg111. Also, it showed five hydrophobic interactions with amino acid residues Glu250, Thr219, His114, Pro491, and Leu254. Additionally, BTP(4) showed two electrostatic interactions with amino acid residue Arg111. The

TABLE 2 Antiproliferative activity of BTP(1), BTP(4), and cisplatin on CT26 and NIH/3T3 cells during 24, 48, and 72 h of treatment.

	IC_{50} (μM) ± SEM (CT26)			IC_{50} (μM) ± SEM (NIH/3T3)		
Compounds	24 (h)	48 (h)	72 (h)	24 (h)	48 (h)	72 (h)
BTP(1)	108.57 ± 5.25	80.71 ± 2.07	37.01 ± 3.58	279.20 ± 10.26	205.98 ± 14.00	197.81 ± 8.37
BTP(4)	110.96 ± 4.03	68.86 ± 4.76	38.92 ± 5.12	231.60 ± 2.17	165.17 ± 2.22	159.92 ± 2.93
Cisplatin	62.56 ± 1.49	18.89 ± 1.03	14.53 ± 0.89	110.92 ± 6.86	40.13 ± 4.59	30.83 ± 2.86

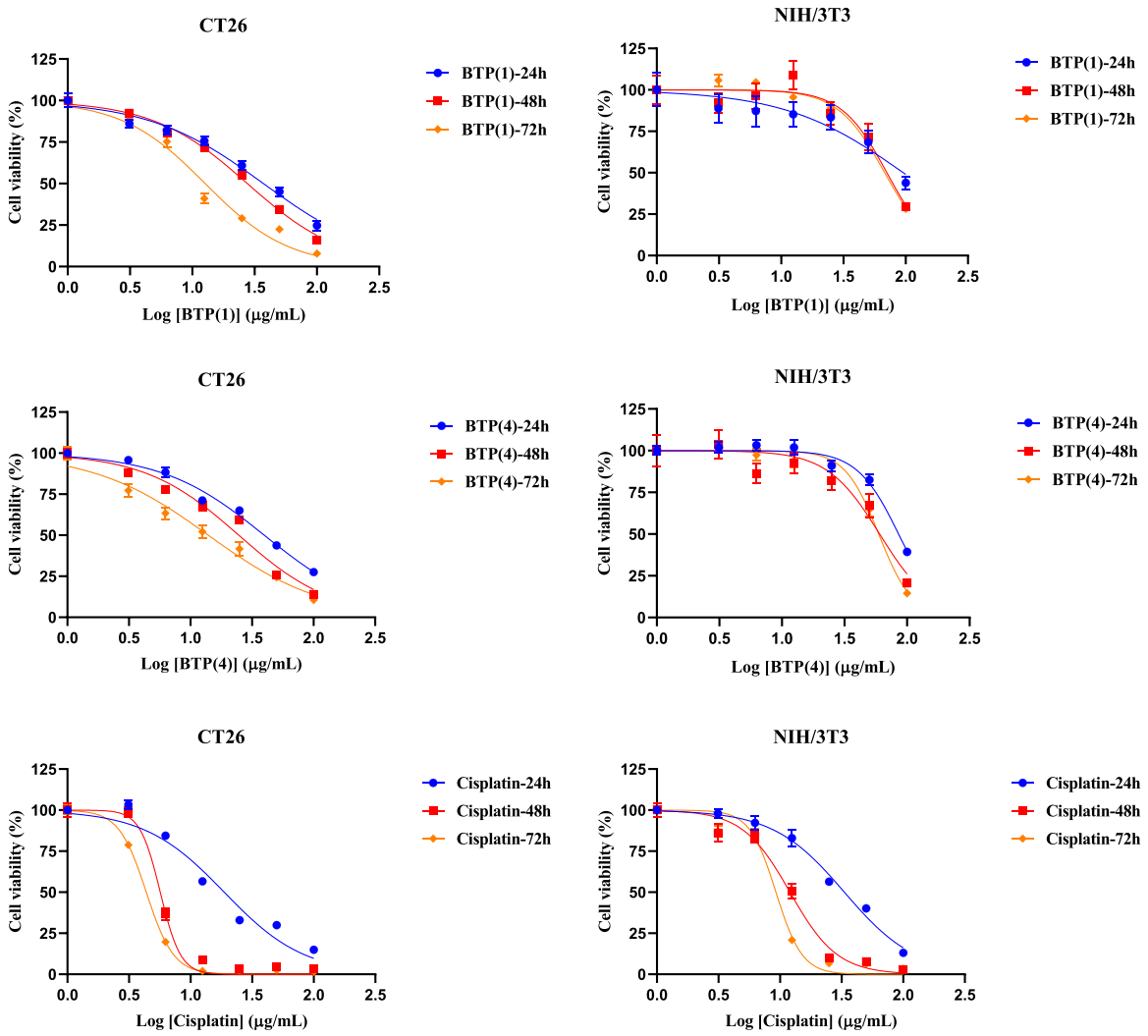

FIGURE 2 Dose–response curves of selected benzothiazolopyrimidines. Anticancer effects of BTP(1), BTP(4), and cisplatin were assessed on CT26 and NIH/3T3 cells using MTT assay. Data are expressed as mean ± SEM, $n = 3$.

antiproliferative effects of BTP(1-6) were first examined on HCT 116 cells since these cells exhibit the highest expression of SHP2 compared to other colorectal cancer cell lines evaluated by the Human Protein Atlas website. IC_{50} values obtained by MTT assay confirmed docking data and indicated that BTP(1) and BTP(4) were more cytotoxic compared to other studied BTP derivatives.

The chlorine atom at the 6 position of benzothiazole nucleus of BTP(1) induces an electron withdrawing effect on benzothiazolopyrimidine. To support the importance of halogen position, a group studied cytotoxic properties of benzothiazole derivatives on HepG2 cells and found three compounds out of nineteen with at least 70% inhibition values.[33] These three benzothiazole derivatives had a similar chlorine atom position to BTP(1), which verifies the crucial position of a chlorine atom for antiproliferative activity. Moreover, the cytotoxicity of BTP(4) can be explained by lipophilic nature and high electronic density of

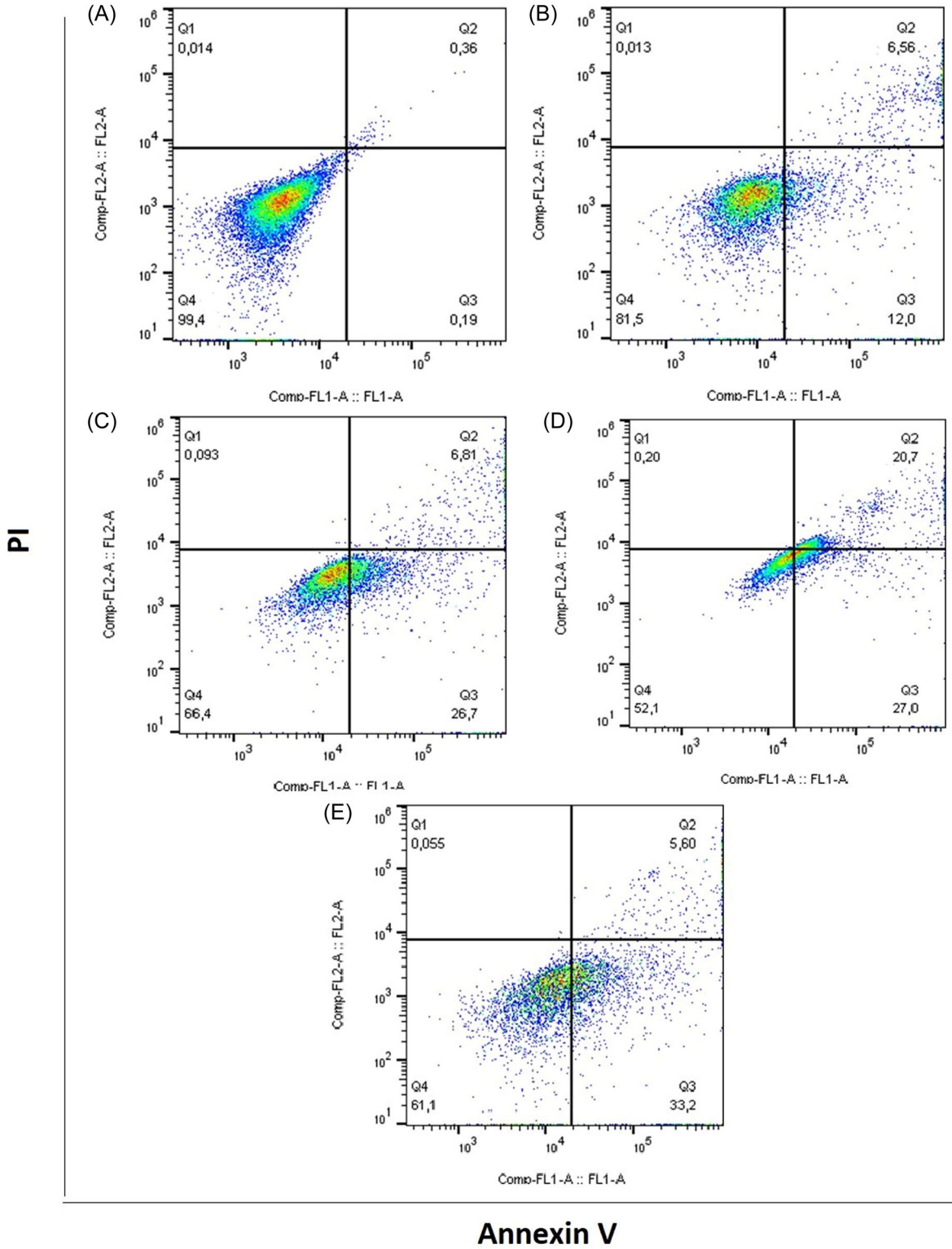

FIGURE 3 Flow cytometry analysis of cell death mechanism induced in treated CT26 cells with selected BTPs after 46 h. (A) Untreated, (B) dimethyl sulfoxide (DMSO), (C) BTP(1) (87.51 μM), (D) BTP(4) (83.78 μM), and (E) cisplatin (16.66 μM) treated cells. The percentage of early apoptotic cells in the BTP derivatives and cisplatin-treated groups compared to controls is considerably higher, which represents the cytotoxic effects of these compounds.

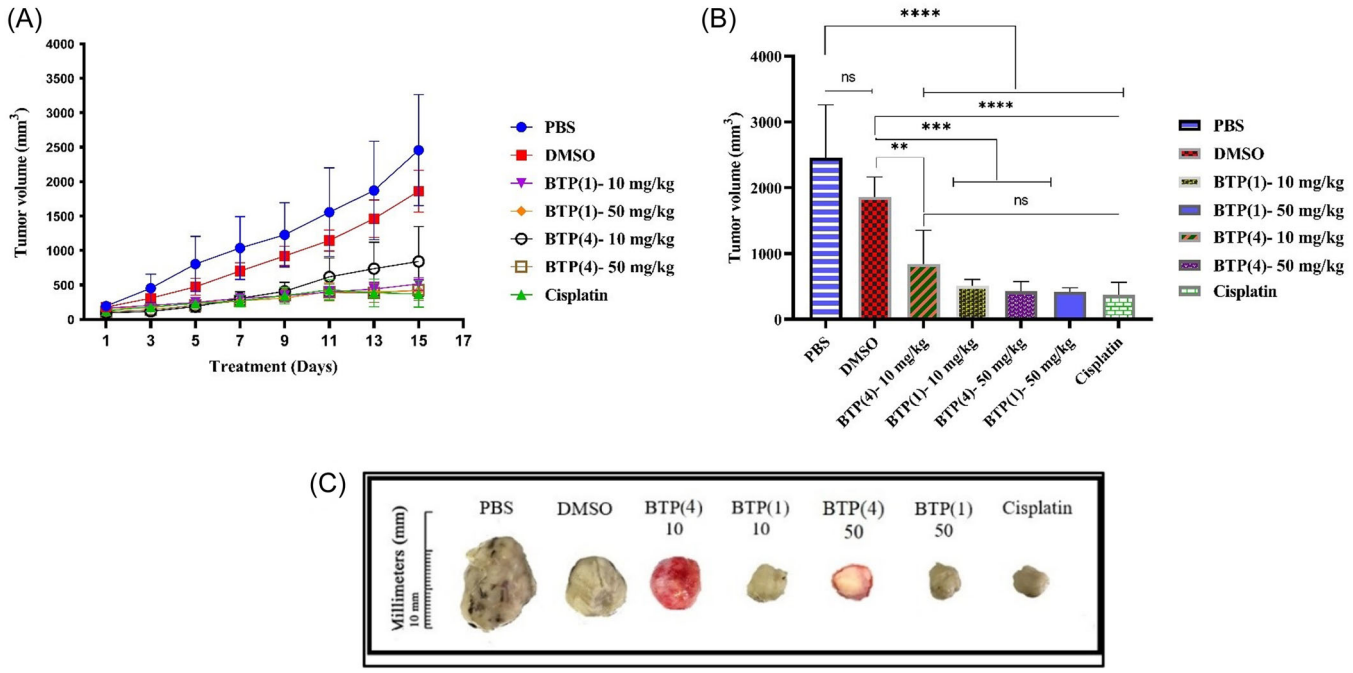

FIGURE 4 In vivo evaluation of selected BTP derivatives on CT26 tumor-bearing BALB/c mice. (A) Tumor growth curves during 15 days of treatment in five groups. Cisplatin, BTP(1), and BTP(4) (both concentrations) demonstrated remarkable antitumor properties. (B) Mean of tumor volume at Day 15 in various groups indicated that cisplatin and both doses of BTP derivatives had a significant difference with control groups (phosphate-buffered saline [PBS] and dimethyl sulfoxide [DMSO]). (C) Representative image of tumors at the end of the experiment. Data are expressed as mean ± SD, $n = 5$. $^{**}p < 0.01$, $^{***}p < 0.001$, $^{****}p < 0.0001$, and ns indicates not significant.

naphthalene, which allows it to permeabilize the lipid membrane and form interactions with cellular proteins.[34] Wilson et al.[35] reported that 1,4-naphthoquinones showed cytotoxic activity against human colon cancer cells such as LoVo, COLO 206, and adenocarcinoma cell lines. In another study, Osowole and colleagues synthesized and evaluated the anticancer activity of complexes with a naphthalene moiety in colon and breast cancer cell lines in vitro. They reported that HT-29 cells were more sensitive to those agents than MCF-7 cells.[36] In general, naphthalene with the molecular formula $C_{10}H_8$ is the simplest bicyclic ring. Owing to its cytotoxic nature, derivatives bearing a naphthalene moiety have several pharmacological implications. These include anticancer,[37-39] antitubercular,[40] anti-HIV,[41] antimicrobial,[42,43] antiviral,[44] and antidiabetic[45] activities. Figure 6 represents the chemical structure of BTP(1) and BTP(4).

The aforementioned reasons led to the selection of the BTP(1) and BTP(4) derivatives as the most potent compounds to evaluate their anticancer effects on CT26 murine colorectal carcinoma cells. Investigating BTP(1) anticancer properties showed significant cytotoxic effects on CT26 compared to NIH/3T3 normal cells (with IC_{50} values of 37.01 and 197.81 µM after 72 h of treatment, respectively, $p < 0.0001$). Interestingly, cytotoxicity of BTP(1) on mouse fibroblast NIH/3T3 was considerably less than that for cisplatin (30.83 µM after 72 h) on these cells ($p < 0.0001$). These results indicate selective toxicity of BTP(1) on CT26 cancerous cells. Furthermore, our results indicated that BTP(4) decreased the viability of CT26 cells (IC_{50} value of 38.92 µM after 72 h of treatment, $p < 0.0001$). Treatment of NIH/3T3 cells with BTP(4) demonstrated that, unlike cisplatin, this compound had a limited effect on these cells (159.92 µM after 72 h). Together, BTP(1) and BTP(4) had significant antitumor activities on CT26 cancer cells.

The cytotoxic effects of BTP(1) have been investigated on acute myeloid leukemia MOLM14 cells.[24] The results of their study showed that BTP(1) reduced the viability of MOLM14 cells with an IC_{50} value of 85 ± 5 µM. BTP(1) was considered an allosteric inhibitor of the protein tyrosine phosphatase SHP2, which through its role in multiple signaling pathways such as RAS–ERK promotes cancer cell proliferation and survival. This study also demonstrated a reduction in the phospho-ERK (p-ERK) level in MOLM14 cells at toxic concentrations of BTP(1). Moreover, cytotoxic effects of BTP(1) were also assessed on A2058 melanoma cells, and it was less efficacious compared to MOLM14 cells. This was explained by the presence of a mutation in *BRAF* gene in A2058 cells, which its product is part of the RAS–ERK signaling pathway. In their study, BTP (1) exhibited a significantly lower yield (15%) compared to our results (89%). The key differences lie in the methodologies: our approach uses a mixture of heterocyclic 1,3-dione, aromatic aldehyde, and o-phenylenediamine in ethanol, stirred at reflux temperature. On the other hand, the method described by LaRochelle et al. involves heating a mixture of 2-amino substituted benzothiazole and diethyl benzylmalonate to 200°C using a microwave synthesizer. Our method employs conventional reflux in ethanol, whereas their approach utilizes microwave-assisted synthesis, typically associated

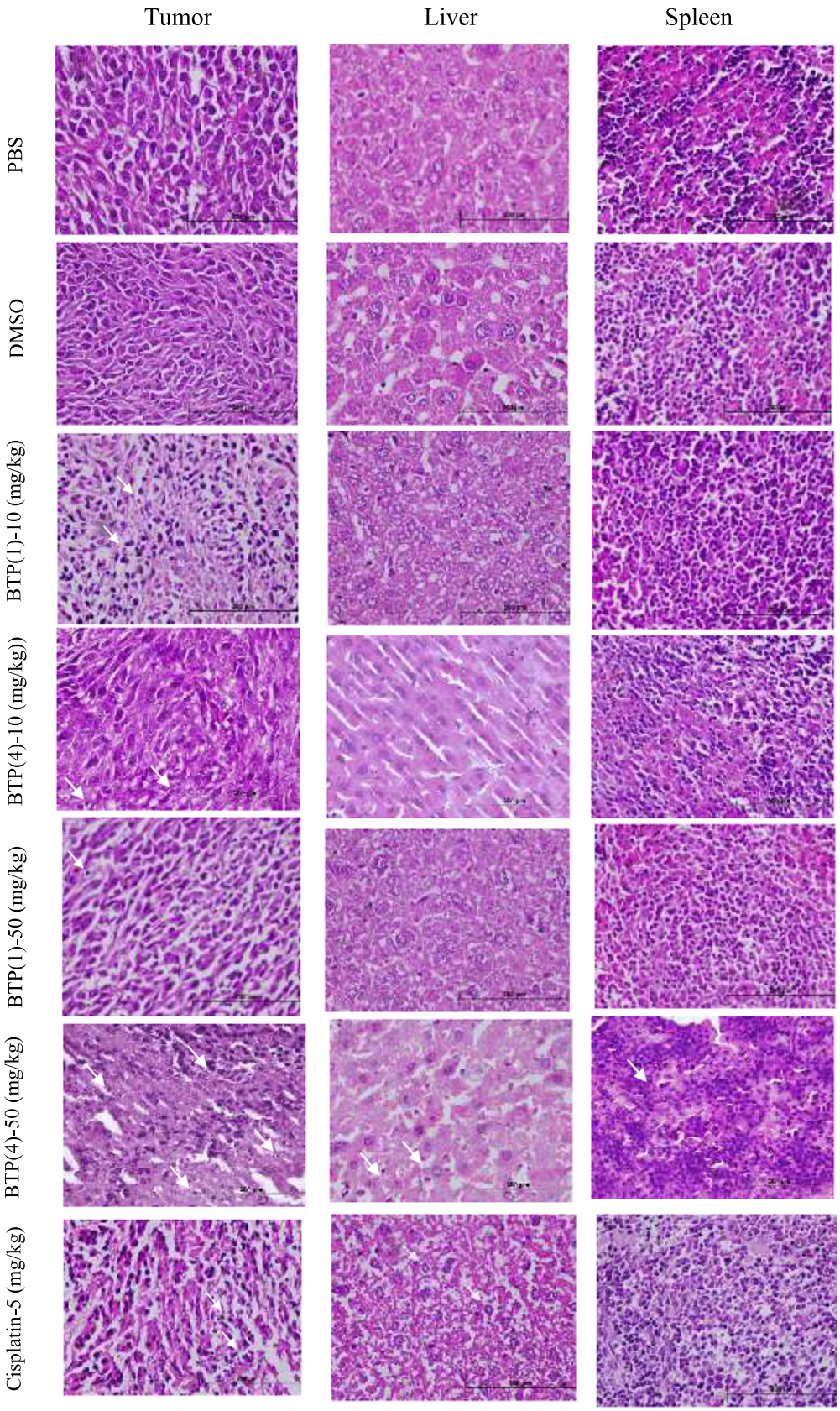

FIGURE 5 Hematoxylin and eosin staining of tumor, liver, and spleen of treated mice collected on Day 15 of treatment. Apoptotic cells and condensed nuclei are observed in BTP(1), BTP(4), and cisplatin-treated groups (tumor section). Damaged hepatocytes and splenocytes with pyknotic nuclei were noticed in cisplatin-treated group and partly in 50 mg/kg of BTP(4). White arrows represent apoptotic and damaged cells. Scale bar: 200 μM.

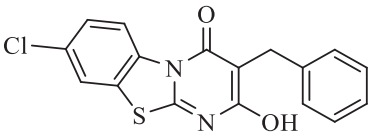

3-benzyl-8-chloro-2-hydroxy-4*H*-benzo[4,5]thiazolo[3,2-*α*]pyrimidin-4-one (BTP(1))

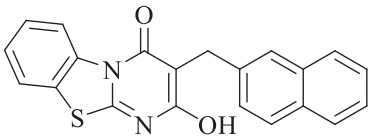

2-hydroxy-3-(naphthalene-2-ylmethyl)-4*H*-benzo[4,5]thiazolo[3,2-*a*]pyrimidin-4-one (BTP(4))

FIGURE 6 Chemical structures and IUPAC names of BTP(1) and BTP(4) derivatives. 3-Benzyl-8-chloro-2-hydroxy-4*H*-benzo[4,5] thiazolo[3,2-*α*]pyrimidin-4-one (BTP(1)). 2-hydroxy-3-(naphthalene-2-ylmethyl)−4*H*-benzo[4,5] thiazolo[3,2-*a*]pyrimidin-4-one (BTP(4)).

with high reaction temperatures. Additionally, our purification process involves filtration, washing, chromatography, and recrystallization. In contrast, their method simplifies purification by directly dissolving the precipitate in boiling ethanol for recrystallization, which is a more rigorous approach.

A possible explanation for the higher cytotoxicity on CT26 compared to HCT 116 after treatment with BTP(1) and BTP(4) might be related to their genotypes. HCT 116 cells harbor mutant *PIK3CA*,[46] while CT26 cells are wild type for *Pik3ca*.[47] Although PI3K-mTORC1 is an independent signaling pathway leading to cell survival and proliferation, it has intense negative and positive cross-talks with the RAS–ERK signaling pathway.[48] As a consequence, considering SHP2 protein as the BTP(1) and BTP(4) target, and with the knowledge that it regulates both RAS–ERK and PI3K–mTORC1[49] signaling pathways as well as their intense cross-talk, *PIK3CA* mutation in HCT 116 cells could be one of the main reasons for cytotoxicity difference in these two cell lines (Figure 7). Further complementary studies are required to confirm these outcomes, especially to elucidate the underlying molecular mechanisms of action of these BTP derivatives.

PI/annexin V-FITC staining was employed to investigate the mechanism of cell death induced by the studied compounds. As depicted in Figure 3, CT26 cells treated with 87.51 μM BTP(1) and 83.78 μM BTP(4) for 46 h showed a significant increase in the percentage of annexin V positive cells, from 18.56% in vehicle control to 33.51% (26.7% early apoptotic plus 6.81% late apoptotic) and 47.7% (27.0% early apoptotic plus 20.7% late apoptotic) in treated cells, respectively, indicating apoptosis as the main cell death mechanism. Similarly, Diao and colleagues[13] carried out a PI/annexin V assay and flow cytometry analysis of HCT 116 cells treated with different concentrations of a benzothiazolopyrimidine derivative. They concluded that the BTP derivative induced apoptosis in HCT 116 cells in a concentration-dependent manner. In the same vein, another study reported a benzothiazole derivative which resulted in the production of a large population of apoptotic cells, 1.2 fold higher than that produced by cisplatin at the same concentration.[50] Together, these studies support apoptosis as the main mechanism of cell death induction by benzothiazolopyrimidine derivatives, however, further research should be undertaken to investigate precise molecular mechanisms inducing apoptosis by these compounds.

To evaluate the efficacy of BTP(1) and BTP(4) as anticancer agents, we expanded our experiments and performed an in vivo assay. Examination of tumor growth during the 15 days follow-up demonstrated that similar to cisplatin (5 mg/kg), both concentrations of BTP(1) and BTP(4), 10 and 50 mg/kg body weight, caused significant regression in tumor growth compared to control groups. Likewise, Yoshida et al.[51] reported 68% tumor inhibition after treating BDF1 mice bearing Lewis lung carcinoma (LLC) with a single dose of 20 mg/kg of a benzothiazole derivative at day 11. Moreover, Shi et al.[52] reported 52% tumor inhibition after treating BDF1 mice bearing human breast carcinoma BO with 20 mg/kg of a benzothiazole derivative. In the present study, treatment with 10 mg/kg BTP(1) and 50 mg/kg BTP(4) inhibited tumor growth by approximately 80% as compared to the PBS group at the end of the experiment (Figure 4). Taken together, these results suggest that BTP(1) and BTP (4) have remarkable inhibitory effects on mouse colorectal carcinoma tumors.

The histological assessments demonstrated that while cisplatin treatment led to a significant decrease in tumor size, it also had adverse side effects in the liver and spleen of treated mice. Evidence suggests that the toxicity of cisplatin in the liver and spleen is dependent on the administered dose. Specifically, as the dose increases, there is a corresponding increase in tissue toxicity.[32] Interestingly, unlike cisplatin, BTP(1) and 10 mg/kg of BTP(4) did not show toxicity in the liver and spleen of treated animals.

Overall, our results suggest that BTP(1) and BTP(4) have remarkable anticancer effects both in vitro and in vivo; and the

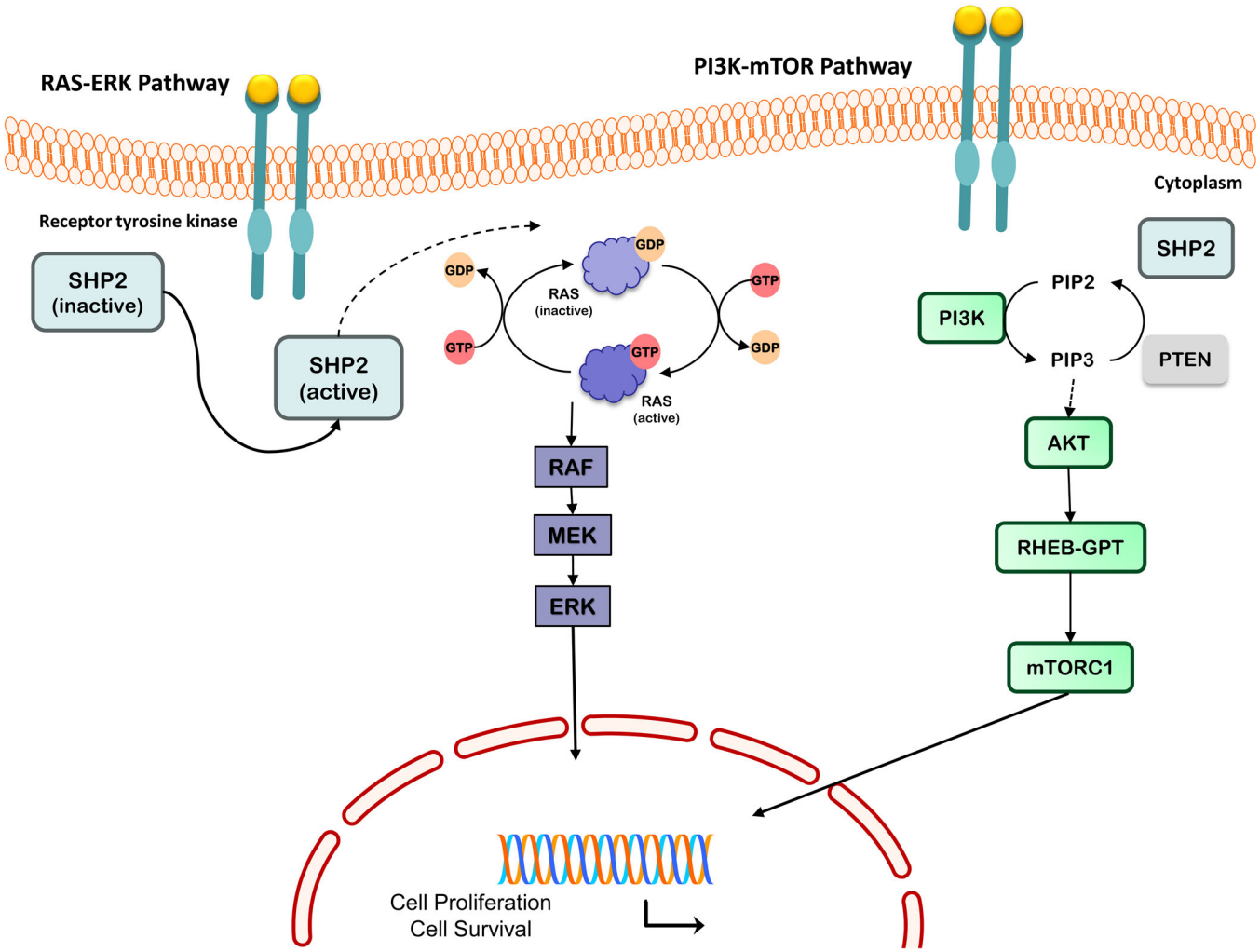

FIGURE 7 The RAS–ERK and PI3K–mTOR signaling pathways are key mechanisms for controlling cell survival, proliferation, and metabolism. These pathways possess strong cross-talk with each other, both positively and negatively. Furthermore, protein tyrosine phosphatase SHP2 can regulate RAS–ERK and PI3K–mTOR pathways and lead to cancer cell survival and division.

mechanism of cell death induced by these BTP derivatives is mainly apoptosis. Although cisplatin suffered from notable side effects both in vitro (on mouse embryonic fibroblast NIH/3T3 cells) and in vivo (liver and spleen lesions of treated mice), BTP(1) and BTP(4) did not demonstrate any serious complications. While these two BTP derivatives may not be optimal as single-agent therapy options, they can be used in combination with conventional CRC treatments, which are often accompanied by side effects. This approach allows for lower therapeutic doses of each drug, thereby minimizing the toxic effects on normal cells while retaining cytotoxic effects on cancer cells. Nevertheless, further investigations are required to elucidate the molecular mechanisms of these BTP derivatives.

AUTHOR CONTRIBUTIONS

Melika Bakharzi: Methodology; writing—original draft; conceptualization; investigation. **Elham Attar**: Conceptualization; writing—original draft; methodology; investigation. **Hossein Garmabi**: Methodology. **Abbas Ali Esmaeili**: Supervision. **Ahmad Reza Bahrami**: Supervision; funding acquisition. **Maryam Danehchin**: Methodology. **Maryam M. Matin**: Conceptualization; funding acquisition; writing—review and editing; methodology; validation; supervision.

ACKNOWLEDGMENTS

This work was supported by Ferdowsi University of Mashhad (grant numbers: 53418 and 53419). The authors would like to thank Dr. Noroozpour laboratory for their technical assistance with tissue processing and Dr. Mahdi Mirahmadi for helping with flow cytometry instrument.

CONFLICT OF INTEREST STATEMENT

The authors declare no conflict of interest.

DATA AVAILABILITY STATEMENT

The data that support the findings of this study are available from the corresponding author upon reasonable request.

ETHICS STATEMENT

All in vivo experiments were conducted under the FUM-approved codes of the care and use of laboratory animals (IR.UM.-REC.1400.052, IR.UM.REC.1400.053).

ORCID

Maryam M. Matin http://orcid.org/0000-0002-7949-7712

REFERENCES

[1] D. Hanahan, R. A. Weinberg, *Cell* **2000**, *100*(1), 57.
[2] H. Sung, J. Ferlay, R. L. Siegel, M. Laversanne, I. Soerjomataram, A. Jemal, F. Bray, *CA Cancer J. Clin.* **2021**, *71*(3), 209.
[3] M. J. Munro, S. K. Wickremesekera, L. Peng, S. T. Tan, T. Itinteang, *J. Clin. Pathol.* **2018**, *71*(2), 110.
[4] E. Dekker, P. J. Tanis, J. L. A. Vleugels, P. M. Kasi, M. B. Wallace, *The Lancet* **2019**, *394*, 1467.
[5] Y. H. Xie, Y. X. Chen, J. Y. Fang, *Signal Transduct. Target Ther.* **2020**, *5*(1), 22.
[6] R. Ali, N. Siddiqui, *J. Chem.* **2013**, *2013*, 1.
[7] N. Pathak, E. Rathi, N. Kumar, S. G. Kini, C. M. Rao, *Mini-Rev. Med. Chem.* **2020**, *20*(1), 12.
[8] D. Ü. Payaz, F. Z. Küçükbay, H. Küçükbay, A. Angeli, C. T. Supuran, *J. Enzyme Inhib. Med. Chem.* **2019**, *34*(1), 343.
[9] A. Irfan, F. Batool, S. A. Zahra Naqvi, A. Islam, S. M. Osman, A. Nocentini, S. A. Alissa, C. T. Supuran, *J. Enzyme Inhib. Med. Chem.* **2020**, *35*(1), 265.
[10] Y. Liu, Y. Wang, G. Dong, Y. Zhang, S. Wu, Z. Miao, J. Yao, W. Zhang, C. Sheng, *MedChemComm* **2013**, *4*(12), 1551.
[11] S. A. F. Rostom, H. M. A. Ashour, H. A. Abd El Razik, *Arch. Pharm.* **2009**, *342*(5), 299.
[12] S. Maddila, S. Gorle, N. Seshadri, P. Lavanya, S. B. Jonnalagadda, *Arabian J. Chem.* **2016**, *9*(5), 681.
[13] P. C. Diao, W. Y. Lin, X. E. Jian, Y. H. Li, W. W. You, P. L. Zhao, *Eur. J. Med. Chem.* **2019**, *179*, 196.
[14] G. S. Waghmare, A. B. Chidrawar, V. N. Bhosale, G. R. Shendarkar, S. V. Kuberkar, *J. Pharmacy Res.* **2013**, *7*(9), 823.
[15] R. M. Kumbhare, T. L. Dadmal, T. A. Devi, D. Kumar, U. B. Kosurkar, D. Chowdhury, K. Appalanaidu, Y. K. Rao, M. J. Ramaiah, M. P. Bhadra, *Med. Chem. Commun.* **2014**, *5*(11), 1744.
[16] J. Zhang, F. Zhang, R. Niu, *J. Cell. Mol. Med.* **2015**, *19*(9), 2075.
[17] H. Chen, S. Libring, K. V. Ruddraraju, J. Miao, L. Solorio, Z. Y. Zhang, M. K. Wendt, *Oncogene* **2020**, *39*(49), 7166.
[18] N. Aceto, N. Sausgruber, H. Brinkhaus, D. Gaidatzis, G. Martiny-Baron, G. Mazzarol, S. Confalonieri, M. Quarto, G. Hu, P. J. Balwierz, M. Pachkov, S. J. Elledge, E. van Nimwegen, M. B. Stadler, M. Bentires-Alj, *Nat. Med.* **2012**, *18*(4), 529.
[19] N. M. Sodir, G. Pathria, J. I. Adamkewicz, E. H. Kelley, J. Sudhamsu, M. Merchant, R. Chiarle, D. Maddalo, *Cancer Discovery* **2023**, *13*(11), 2339.
[20] D. Chen, H. B. Barsoumian, L. Yang, A. I. Younes, V. Verma, Y. Hu, H. Menon, M. Wasley, F. Masropour, S. Mosaffa, T. Ozgen, K. Klein, M. A. Cortez, J. W. Welsh, *Cancer Immunol. Res.* **2020**, *8*(7), 883.
[21] Y. Huang, J. Wang, F. Cao, H. Jiang, A. Li, J. Li, L. Qiu, H. Shen, W. Chang, C. Zhou, Y. Pan, Y. Lu, *Sci. Rep.* **2017**, *7*(1), 17597.
[22] M. Yu, C. Xu, H. Zhang, J. Lun, L. Wang, G. Zhang, J. Fang, *Biochem. Biophys. Res. Commun.* **2021**, *563*, 1.
[23] J. Gao, Z. Wu, M. Zhao, R. Zhang, M. Li, D. Sun, H. Cheng, X. Qi, Y. Shen, Q. Xu, H. Chen, D. Chen, Y. Sun, *Acta Pharm. Sin. B* **2022**, *12*(1), 149.
[24] J. R. LaRochelle, M. Fodor, J. M. Ellegast, X. Liu, V. Vemulapalli, M. Mohseni, T. Stams, S. J. Buhrlage, K. Stegmaier, M. J. LaMarche, M. G. Acker, S. C. Blacklow, *Bioorg. Med. Chem.* **2017**, *25*(24), 6479.
[25] M. Danehchin, A. A. Esmaeili, *Mol. Divers.* **2022**, *26*(2), 1191.
[26] J. Van Meerloo, G. J. Kaspers, J. Cloos, *Cancer Cell Culture: Methods and Protocols*, Springer, **2011**, p. 237.
[27] N. Arghiani, M. M. Matin, A. R. Bahrami, M. Iranshahi, A. Sazgarnia, F. B. Rassouli, *Life Sci.* **2014**, *109*(2), 87.
[28] V. MabTag Annexin Apoptosis Detection Kit. https://www.mabtag.com/MabTag_Data_sheet_Annexin-Kit_08-2017.pdf
[29] E. Ojo-Amaize, *World J. Gastroenterol.* **2007**, *13*(34), 4586.
[30] R. L. Siegel, K. D. Miller, H. E. Fuchs, A. Jemal, *CA Cancer J. Clin.* **2022**, *72*, 7.
[31] R. Hickey, M. Vouche, D. Y. Sze, E. Hohlastos, J. Collins, T. Schirmang, K. Memon, R. K. Ryu, K. Sato, R. Chen, R. Gupta, S. Resnick, J. Carr, H. B. Chrisman, A. A. Nemcek, R. L. Vogelzang, R. J. Lewandowski, R. Salem, *J. Vasc. Interv. Radiol.* **2013**, *24*(8), 1167.
[32] S. Dasari, P. Bernard Tchounwou, *Eur. J. Pharmacol.* **2014**, *740*, 364.
[33] F. Corbo, A. Carocci, D. Armenise, N. De Laurentis, A. Laghezza, F. Loiodice, P. Ancona, M. Muraglia, V. Pagliarulo, C. Franchini, A. Catalano, *J. Chem.* **2016**, *2016*, 1.
[34] S. Makar, T. Saha, S. K. Singh, *Eur. J. Med. Chem.* **2019**, *161*, 252.
[35] G. D. Wilson, M. d'Arcy Doherty, G. M. Cohen, *Br. J. Cancer* **1985**, *51*(6), 853.
[36] A. A. Osowole, A. A. Oni, K. Onyegbula, A. T. Hassan, *Int. Res. J. Pure Appl. Chem.* **2012**, *2*(3), 211.
[37] K. Vogel, J. Sterling, Y. Herzig, A. Nudelman, *Tetrahedron* **1996**, *52*(8), 3049.
[38] R. F. Luduena, M. C. Roach, P. Horowitz, *Biochim. Biophys. Acta* **1986**, *873*(1), 143.
[39] S. Valente, D. Trisciuoglio, T. De Luca, A. Nebbioso, D. Labella, A. Lenoci, C. Bigogno, G. Dondio, M. Miceli, G. Brosch, D. Del Bufalo, L. Altucci, A. Mai, *J. Med. Chem.* **2014**, *57*(14), 6259.
[40] M. Asif, *World J. Organ. Chem.* **2013**, *1*(2), 14.
[41] H. Zhang, D. Soejarto, L. Rong, H. H. S. Fong, Rumschlag-Booms E. inventors; University of Illinois, assignee. Aryl naphthalide lignans as anti-hiv agents. United States Patent Application US *14/235*,870. **2014**.
[42] Y. Y. Chen, L. Gopala, R. R. Y. Bheemanaboina, H. B. Liu, Y. Cheng, R. X. Geng, C. H. Zhou, *ACS Med. Chem. Lett.* **2017**, *8*(12), 1331.
[43] G. Laverty, A. P. McCloskey, B. F. Gilmore, D. S. Jones, J. Zhou, B. Xu, *Biomacromolecules* **2014**, *15*(9), 3429.
[44] A. K. Debnath, L. Radigan, S. Jiang, *J. Med. Chem.* **1999**, *42*(17), 3203.
[45] É. Bokor, S. Kun, D. Goyard, M. Tóth, J. P. Praly, S. Vidal, L. Somsák, *Chem. Rev.* **2017**, *117*(3), 1687.
[46] D. Ahmed, P. W. Eide, I. A. Eilertsen, S. A. Danielsen, M. Eknæs, M. Hektoen, G. E. Lind, R. A. Lothe, *Oncogenesis* **2013**, *2*(9), e71.
[47] J. C. Castle, M. Loewer, S. Boegel, J. de Graaf, C. Bender, A. D. Tadmor, V. Boisguerin, T. Bukur, P. Sorn, C. Paret, M. Diken, S. Kreiter, Ö. Türeci, U. Sahin, *BMC Genomics* **2014**, *15*, 190.
[48] M. C. Mendoza, E. E. Er, J. Blenis, *Trends Biochem. Sci.* **2011**, *36*(6), 320.
[49] X. Yuan, H. Bu, J. Zhou, C. Y. Yang, H. Zhang, *J. Med. Chem.* **2020**, *63*(20), 11368.
[50] F. Eshkil, H. Eshghi, A. S. Saljooghi, M. Bakavoli, M. Rahimizadeh, *Russ. J. Bioorg. Chem.* **2017**, *43*, 576.
[51] M. Yoshida, I. Hayakawa, N. Hayashi, T. Agatsuma, Y. Oda, F. Tanzawa, S. Iwasaki, K. Koyama, H. Furukawa, S. Kurakata, Y. Sugano, *Bioorg. Med. Chem. Lett.* **2005**, *15*(14), 3328.

[52] D. F. Shi, T. D. Bradshaw, S. Wrigley, C. J. McCall, P. Lelieveld, I. Fichtner, M. F. G. Stevens, *J. Med. Chem.* **1996**, *39*(17), 3375.

SUPPORTING INFORMATION

Additional supporting information can be found online in the Supporting Information section at the end of this article.

How to cite this article: M. Bakharzi, E. Attar, H. Garmabi, A. A. Esmaeili, A. R. Bahrami, M. Danehchin, M. M. Matin, *J. Biochem. Mol. Toxicol.* **2024**, *38*, e23779. https://doi.org/10.1002/jbt.23779